Int J Thermophys (2010) 31:475–487
DOI 10.1007/s10765-010-0757-1

Hot-Wire Method for Kinematic Viscosity Estimation

Valter Giaretto

Received: 18 June 2009 / Accepted: 13 May 2010 / Published online: 1 June 2010

Abstract This paper explores the characterization of thermal and momentum diffusion properties of condensed phase biological fluids. The widely used transient hot-wire technique for determination of thermal diffusion properties is proposed here to investigate also the apparent kinematic viscosity of fluids with the apparatus commonly adopted for thermal conductivity and/or thermal diffusivity determination. The undesired onset of convection in the determination of thermal diffusion properties is in this case the useful effect measured at the wire–fluid interface. From a theoretical point of view, the onset of convection time at a given vertical position along the wire has been related to the Prandtl number, and the reliability of the kinematic viscosity has been studied and preliminarily tested in the case of water.

Keywords Free convection · Hot-wire method · Kinematic viscosity · Onset of convection · Prandtl number

1 Introduction

In the transient hot-wire technique the onset of free convection, the absorption and emission of radiation from the heated fluid, and the axial conduction due to the finite length of the wire can induce a remarkable deviation (several percent) from the pure

V. Giaretto (✉)
Dipartimento di Energetica, Politecnico di Torino, C.so Duca degli Abruzzi, 24, 10129 Torino, Italy
e-mail: valter.giaretto@polito.it

V. Giaretto
Consorzio Nazionale Interuniversitario di Scienze fisiche della Materia (CNISM), Unità di Ricerca Politecnico di Torino, C.so Duca degli Abruzzi, 24, 10129 Torino, Italy

radial conduction regime. The wire temperature rise deviates in this case from the ideal linear trend in a semi-log plot.

The influence of axial conduction becomes negligible if the length of the wire (usually made of platinum) is greater than a thousand times its radius [1]. The way of avoiding the wire end effect is to place the current leads at the wire ends and the potential leads at a sufficient distance from the wire ends, that is, at about one hundred times the wire diameter [2,3]. A pronounced radiation contribution is present for strong absorbing liquids and for large temperature ranges. In this case, several useful corrections of the wire measurement temperature are reported in the literature [4–6].

The influence of free convection limits the experimental time that is useful to estimate the thermal diffusion properties, and beyond which, measurements are affected by a mixed conduction and convection regime. The transient free convection along vertical circular cylinders has been dealt with in both past and recent literature. Goldstein and Briggs [7] made a theoretical analysis of transient free convection for vertical circular cylinders immersed in an infinite medium, initially at rest. They considered the cylinder as a perfect heat conductor, with or without a finite heat capacity, and producing a step change in the surface heat flux giving analytical solutions for arbitrary Prandtl numbers. Pantaloni et al. [8] experimentally studied the onset of free convection in a hot-wire apparatus, stating by means of Schlieren-type visualization, that the boundary layer is clearly dominant in the fluid motion and showed the absence of a radial velocity component, as stated by Goldstein and Briggs. Velusamy and Garg [9] and De Lorenzo and Padet [10] numerically investigated transient free convection along a vertical cylindrical and flat surfaces, respectively, adopting a physical model that is analogous to the approach recommended by Goldstein and Briggs.

No correction for the convection effect is usually considered in the hot-wire method to eliminate this influence from the measurements. Typically, the onset of convection time is determined to avoid the convection effect in measurements [11], so that the part of the transient determined only by a conduction regime can be considered. Consequently, the possibility of describing free convection development at the wire–fluid interface could enable the fluid properties related to momentum diffusion to be investigated.

The aim of this work was to investigate a correlation between the fluid motion in the wire vicinity, the onset of convection time at the wire–fluid interface, and the apparent kinematic viscosity of the fluid. Once this approach is demonstrated with general purpose hot-wire experiments, it can be applied to the phase of condensed biological fluids, in particular, hematic compounds. In this field, the interest is to study hematic thermal and momentum diffusion properties at low shear rates and low velocities, so the hot-wire technique could be suitable for this purpose. The approach introduced by Goldstein and Briggs for predicting when the influence of the leading edge will penetrate a given vertical distance was adopted. The transient development of free convection enables the introduction of the onset of convection time as a parameter useful to estimate the apparent kinematic viscosity of condensed phase fluids. A sensitivity analysis is proposed in order to evaluate the uncertainty of this property, and an example for the determination of the onset of convection time and the Prandtl number is reported, by using measurements performed on water.

2 Mathematical Model

To predict the onset of free convection, the boundary layer assumption in the governing equations has been considered. The hot wire was assumed as a semi-infinite vertical circular cylinder, so, neglecting the vertical conduction in the wire and the fluid across the leading edge, unsteady one-dimensional solutions for temperature and velocity fields were taken into account. As is usual in the case of slow free convection, the viscous dissipation terms in the momentum equation, and the density variation in the continuity equation, were neglected; the density influence was only considered in the buoyancy term (Boussinesq approximation).

A step change of heat generation in the cylinder causes a perturbation in the surrounding fluid that behaves like a wave rising from the leading edge. At a given position along the vertical wire (z direction in our case), the transition from pure conduction to mixed conduction and convection occurs when the fluid moving up reaches this position. A uniform wall temperature of the wire above the leading edge takes place for constant and uniform heat generation. With these conditions, both the temperature and the vertical velocity are only dependent on the time and radial position; they are independent of z and, therefore, according to the continuity equation, no velocity takes place in the radial direction. By integrating the vertical velocity with respect to time, the wave propagation inside the fluid gives the penetration distance $Z(r, t)$ from the convection leading edge as a function of the time t and the radial position r. At a given time, the maximum distance of the fluid moving up from the leading edge determines the maximum penetration distance $\hat{Z}(t)$, where the convection effect takes place, whatever radial position it reaches first.

On this basis, transient one-dimensional heat transfer is due to pure conduction and momentum equations can be adopted before the effects from the leading edge have propagated to a given vertical position in the fluid. Introducing the dimensionless temperature difference ϑ between the wire and the undisturbed fluid, with the thermal conductivity λ of the fluid and the heat rate q generated inside the wire per unit length, assuming the wire as a perfect heat conductor with a finite heat capacity, adopting a cylindrical coordinate system, the dimensionless temperature field is given by [12]

$$\vartheta(\xi, \tau, \delta) = \frac{\lambda(T - T_\infty)}{q} = \frac{1}{\pi^2} \int_0^\infty \left[1 - \exp\left(-\tau\psi^2\right)\right] \frac{\varepsilon(\xi, \delta, \psi)}{\phi(\delta, \psi)} \frac{\mathrm{d}\psi}{\psi^2}, \tag{1}$$

where

$$\varepsilon(\xi, \delta, \psi) = Y_0(\xi\psi)J_1(\psi) - J_0(\xi\psi)Y_1(\psi) + \left\{\frac{\psi}{2\delta}\left[J_0(\xi\psi)Y_0(\psi) - Y_0(\xi\psi)J_0(\psi)\right]\right\} \tag{2}$$

$$\phi(\delta, \psi) = Y_1^2(\psi) + J_1^2(\psi) + \left\{\left(\frac{\psi}{2\delta}\right)^2 \left[Y_0^2(\psi) + J_0^2(\psi)\right] - \frac{\psi}{\delta}\left[Y_0(\psi)Y_1(\psi) + J_0(\psi)J_1(\psi)\right]\right\}. \tag{3}$$

The quantities $\xi = r/r_0$ and $\tau = at/r_0^2$, both referring to the hot-wire radius r_0, are the dimensionless radial position and Fourier number, respectively, whereas a is the thermal diffusivity of the fluid and δ is the ratio of the heat capacity per unit volume of the fluid to that of the wire. $J_k(-)$ and $Y_k(-)$ in Eqs. 2 and 3 are the well-known Bessel functions of order k, of the first and second kind, respectively, and ψ is a dummy real integration variable.

As far as the fluid velocity field is concerned, if the viscous dissipation terms and pressure work are also neglected, the dimensionless momentum equation is written as

$$\frac{\partial^2 \upsilon}{\partial \xi^2} + \frac{1}{\xi}\frac{\partial \upsilon}{\partial \xi} + \frac{\vartheta(\xi, \tau, \delta)}{Pr} = \frac{1}{Pr}\frac{\partial \upsilon}{\partial \tau} \qquad \forall \xi \geq 1, \tag{4}$$

where $\upsilon = w\lambda a/(g\beta q r_0^2)$ is the dimensionless z component of the velocity w, β is the isobaric thermal expansion coefficient, g is the acceleration due to the body force, and Pr is the Prandtl number. For Pr values different from one, the solution for Eq. 4 is given by [7]

$$\upsilon(\xi, \tau, Pr, \delta) = \frac{1}{\pi^2 (Pr-1)} \int_0^\infty \left[\tau\psi^2 + \exp\left(-\tau\psi^2\right) - 1\right] \frac{\chi(\xi, Pr, \delta, \psi)}{\varphi(Pr, \delta, \psi)} \frac{\mathrm{d}\psi}{\psi^4}. \tag{5}$$

Setting $\eta = \psi Pr^{-0.5}$, functions χ and ϕ are

$$\begin{aligned}\chi(\xi, Pr, \delta, \psi) = {} & [Y_1(\psi) Y_0(\psi) + J_1(\psi) J_0(\psi)][Y_0(\xi\eta) J_0(\eta) - J_0(\xi\eta) Y_0(\eta)] \\ & + \left[J_0^2(\eta) + Y_0^2(\eta)\right][Y_1(\psi) J_0(\xi\psi) - J_1(\psi) Y_0(\xi\psi)] \\ & + \frac{2}{\pi\psi}[J_0(\xi\eta) J_0(\eta) + Y_0(\xi\eta) Y_0(\eta)] \\ & + \left\{\frac{\psi}{2\delta}\left[J_0^2(\eta) + Y_0^2(\eta)\right][J_0(\psi) Y_0(\xi\psi) - Y_0(\psi) J_0(\xi\psi)]\right. \\ & \left. + \frac{\psi}{2\delta}\left[J_0^2(\psi) + Y_0^2(\psi)\right][J_0(\xi\eta) Y_0(\eta) - Y_0(\xi\eta) J_0(\eta)]\right\},\end{aligned} \tag{6}$$

and

$$\begin{aligned}\varphi(Pr, \delta, \psi) = {} & \left[J_1^2(\psi) + Y_1^2(\psi)\right]\left[J_0^2(\eta) + Y_0^2(\eta)\right] \\ & + \left\{\frac{\psi^2}{4\delta^2}\left[J_0^2(\eta) + Y_0^2(\eta)\right]\left[J_0^2(\psi) + Y_0^2(\psi)\right] - \right. \\ & \left. + \frac{\psi}{\delta}\left[J_0^2(\eta) + Y_0^2(\eta)\right][J_0(\psi) J_1(\psi) + Y_0(\psi) Y_1(\psi)]\right\}.\end{aligned} \tag{7}$$

Integrating the dimensionless velocity of Eq. 5 with respect to the Fourier number τ, the dimensionless vertical penetration distance ζ becomes

$$\begin{aligned}\zeta\,(\xi,\tau,Pr,\delta) &= \frac{Z\lambda a^2}{g\beta q r_0^4} = \int_0^{\tau} \upsilon\,(\xi,\tau,Pr,\delta)\mathrm{d}\tau \\ &= \frac{1}{\pi^2\,(Pr-1)} \int_0^{\infty} \left[1-\tau\psi^2+\frac{\tau^2\psi^4}{2}-\exp\left(-\tau\psi^2\right)\right] \frac{\chi\,(\xi,Pr,\delta,\psi)}{\varphi(Pr,\delta,\psi)} \frac{\mathrm{d}\psi}{\psi^6}.\end{aligned} \tag{8}$$

For given values of τ, Pr, and δ, the radial dimensionless position, $\hat{\xi}$, where the maximum dimensionless penetration distance, $\hat{\zeta}$, occurs is obtained by imposing the null value of the first derivative of Eq. 8 with respect to the dimensionless radial position ξ:

$$\int_0^{\infty} \left[1-\tau\psi^2+\frac{\tau^2\psi^4}{2}-\exp\left(-\tau\psi^2\right)\right] \frac{\hat{\chi}(\hat{\xi},Pr,\delta,\psi)}{\varphi(Pr,\delta,\psi)} \frac{\mathrm{d}\psi}{\psi^6} = 0, \tag{9}$$

where

$$\begin{aligned}\hat{\chi}(\hat{\xi},Pr,\delta,\psi) = {} & \eta\,[Y_1(\psi)\,Y_0(\psi)+J_1(\psi)\,J_0(\psi)]\left[J_1\left(\hat{\xi}\eta\right)Y_0(\eta)-Y_1\left(\hat{\xi}\eta\right)J_0(\eta)\right] \\ & +\psi\left[J_0^2(\eta)+Y_0^2(\eta)\right]\left[J_1(\psi)\,Y_1\left(\hat{\xi}\psi\right)-Y_1(\psi)\,J_1\left(\hat{\xi}\psi\right)\right] \\ & -\frac{2\eta}{\pi\psi}\left[J_1\left(\hat{\xi}\eta\right)J_0(\eta)+Y_1\left(\hat{\xi}\eta\right)Y_0(\eta)\right] \\ & +\left\{\frac{\psi^2}{2\delta}\left[J_0^2(\eta)+Y_0^2(\eta)\right]\left[Y_0(\psi)\,J_1\left(\hat{\xi}\psi\right)-J_0(\psi)\,Y_1\left(\hat{\xi}\psi\right)\right]\right. \\ & \left.+\frac{\psi\eta}{2\delta}\left[J_0^2(\psi)+Y_0^2(\psi)\right]\left[Y_1\left(\hat{\xi}\eta\right)J_0(\eta)-J_1\left(\hat{\xi}\eta\right)Y_0(\eta)\right]\right\}.\end{aligned} \tag{10}$$

Solutions for Eq. 9 were obtained by using a bisection method, and calculation of the previous improper integrals was carried out numerically through successive iterations, using the Romberg algorithm with an open formula.

Trends for $\ln\hat{\zeta}$ versus $\ln\tau$ are shown in Fig. 1, for Prandtl numbers ranging between 2 and 1000, assuming $\delta = 1$. As evident in this figure, the maximum vertical penetration distance is decreasing with increasing Prandtl number, and a quite linear trend versus $\ln\tau$ is found independent of the Prandtl number chosen. Higher correlation could be obtained by using a polynomial in $\ln\tau$ of higher order.

The influence of the wire heat capacity is appreciable close to the wire surface for small τ values ($\tau < 10$). The vertical penetration distance increases with δ, for δ val-

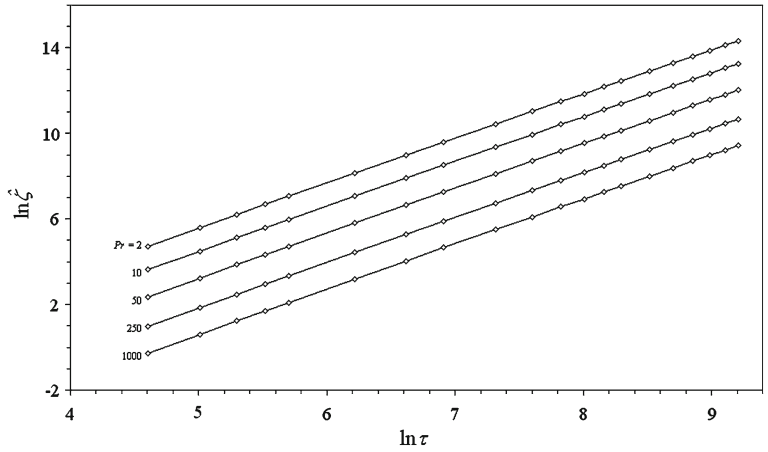

Fig. 1 Maximum dimensionless vertical penetration distance versus Fourier number, for various Prandtl number values

ues between 0.5 and 1.5, and τ values greater than 1000; the maximum influence of δ vanishes, when the Prandtl numbers ranges between 2 and 1000. When large values of δ are applicable (negligible heat capacity of the wire), the terms in the double brackets of Eqs. 2, 3, 6, 7, and 10 can be omitted.

3 Kinematic Viscosity Estimation and Uncertainty

Let us consider a vertical wire, surrounded by an isothermal fluid at rest. Assuming that the electrical current leads are placed at the wire ends and a few measurement zones are positioned along the wire as shown in Fig. 2, when a step change in surface heat flux is produced by feeding the wire, the transient free convection phenomenon begins from the lower leading edge ($z = 0$ in Fig. 2). Neglecting axial conduction along the wire and the fluid, after the correction from the radiation contribution for the case of an absorbing fluid, and before the onset of convection at a given vertical position, measurements are driven only by pure radial conduction. This transient regime ends when the fluid that is moving upwards reaches the vertical position $Z_{\mathrm{low},j}$ corresponding to the lower potential lead of the jth measurement zone, then a mixed conduction and convection regime takes place in this zone.

For each measurement zone along the wire, the experiment can therefore be divided into two parts: one before and another after the onset of free convection. In the absence of convection effects, the first part of the experiment is suitable, as is well known, to evaluate the thermal diffusion properties, the thermal conductivity, the thermal diffusivity, or the volumetric heat capacity; whereas, after the onset of convection, the onset time can be related to the momentum diffusion properties, such as the apparent kinematic viscosity.

As shown in the mathematical modeling section, the development of natural convection is related to the vertical penetration distance from the lower leading edge by

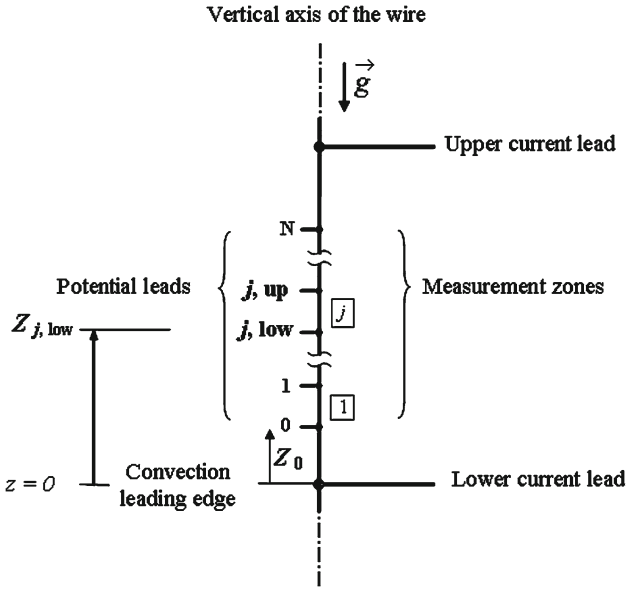

Fig. 2 Schematic diagram of the hot-wire arrangement with the positions of the measurement zones, and the potential and current leads

a dimensionless function ζ of the radial position ξ and Fourier number τ, with Pr and δ as parameters. For a given value of these parameters, at a given τ, the vertical penetration distance presents a maximum value $\hat{\zeta}$ at the radial position corresponding to $\hat{\xi}$. As mentioned in the mathematical modeling section, $\hat{\zeta}$ is weakly dependent on the wire heat capacity, especially when the Fourier number is large, as is the case for a typical wire made of platinum. To cover a wide range of fluid heat capacity, δ should be fixed within 0.5 to 1.5. Since the Fourier number refers to the onset of convection time t_C at the maximum reaching vertical position $\hat{\zeta}$, it is possible to find a relation where the Prandtl number (i.e., the kinematic viscosity) is the parameter to be estimated:

$$\hat{\zeta} = f(\tau, Pr). \tag{11}$$

A first approximation of Eq. 11 stands for a power function of the Fourier number, for whichever Prandtl number in the range 2 to 1000 is chosen. In this way, an approximate value $\tilde{\zeta}$ for the maximum penetration distance is given by the following expression:

$$\ln \tilde{\zeta} = g(Pr) + h(Pr) \ln \tau, \tag{12}$$

where

$$g(Pr) = \sum_{k=0}^{M} G_k \ln^k (Pr), \quad h(Pr) = \sum_{k=0}^{N} H_k \ln^k (Pr), \tag{13}$$

Table 1 Coefficients for Eq. 13 obtained by regression

k	G_k	H_k
0	-4.33337	2.07182
1	-5.58775×10^{-1}	2.40067×10^{-3}
2	-4.61448×10^{-2}	-1.37229×10^{-4}
3	1.92572×10^{-3}	1.17049×10^{-5}

are functions of the sole Prandtl number. The coefficients G_k and H_k has been determined by nonlinear regression on the $\hat{\zeta}$ values obtained from Eq. 9, solved for several values of the Prandtl number in the range 2 to 1000 and Fourier number in the range 100 to 10000. The maximum likelihood values were obtained assigning $M = N = 3$ with the coefficients G_k and H_k reported in Table 1.

The identification of the kinematic viscosity (i.e., the Prandtl number) is strictly related to the sensitivity of the measurement of the onset of convection time t_C at a given vertical position along the wire. A sensitivity coefficient is in this case introduced by means of the first partial derivative of the Fourier number with respect to the Prandtl number. Considering the approximate relation for the maximum penetration distance introduced by Eq. 12, it results in

$$\frac{\partial \tau}{\partial Pr} = -\frac{\tau}{h(Pr)}\left[\frac{\partial g(Pr)}{\partial Pr} + \ln \tau \frac{\partial h(Pr)}{\partial Pr}\right]. \tag{14}$$

Taking into account Eq. 13, the sensitivity coefficient is assumed to be the ratio between the relative uncertainty on the experimental determination of the onset of convection time and the relative uncertainty on the Prandtl number estimation, and is written as

$$\begin{aligned}\frac{Pr}{\tau}\frac{\partial \tau}{\partial Pr} &= -\frac{1}{h(Pr)}\left[\sum_{k=0}^{M-1}(k+1)\,G_{k+1}\ln^k(Pr) + \ln\tau \sum_{k=0}^{N-1}(k+1)\,H_{k+1}\ln^k(Pr)\right] \\ &= \frac{u_{t_C}}{u_{Pr}}.\end{aligned} \tag{15}$$

With the coefficients of Table 1, the calculated sensitivity increases in proportion to the Prandtl number and it is weakly dependent on τ, as shown in Fig. 3. By choosing a constant value versus τ for the calculated sensitivity coefficient, and expecting for the Prandtl number estimation the same uncertainty as for the thermal diffusivity, the relative uncertainty u_ν in the kinematic viscosity determination has the same order of u_{t_C}, and it is expected to be in the range

$$3.2u_{t_C} < u_\nu < 4.9u_{t_C}. \tag{16}$$

The uncertainty in the determination of the onset time t_C depends on the time resolution of the experiment, but it also depends on both the uncertainty of the measured temperature and the rate of deviation in temperature caused by the convection onset with respect to the pure conduction regime. As is known [12], the trend of the dimensionless temperature ϑ, for $4\tau \gg 1$ can be suitably approximated by

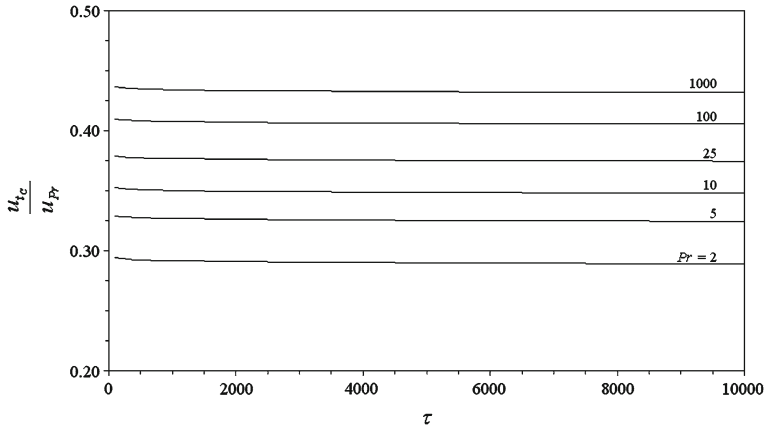

Fig. 3 Ratio between the relative uncertainty of the estimated onset time and the relative uncertainty in the Prandtl number determination versus the Fourier number

$$\vartheta = \frac{1}{4\pi}\ln\left(\frac{4\tau}{\gamma}\right) = x \qquad \forall x \gg \frac{1}{4\pi}\ln\left(1/\gamma\right), \tag{17}$$

where γ is the exponential of Euler's constant. For a pure conduction regime, ϑ is a linear function versus the independent variable x. In the experiments, the deviation from linearity due to convection onset can be established in a statistical way by introducing the ratio $\Im$ between the expected and unexpected square residual (F-test). When the pure conduction regime occurs, the estimated standard deviation S_ϑ depends only on the measurement uncertainty of the temperature, and, for measurement uncertainty randomly distributed, it can be assumed as a constant and independent of x; in this case $\Im$ increases in a monotonic way. Otherwise, when the convection effect take place, the deviation of ϑ from a linear trend increases S_ϑ in a nonrandom manner, so $\Im$ changes its growing trend and begins to decrease rather abruptly.

Since ϑ is a continuous function versus x, for x values ranging between X_0, the minimum value which satisfies the condition imposed for suitable uses of Eq. 17, and an arbitrary value $X > X_0$, the ratio $\Im$ can be written as

$$\Im = \frac{1}{S_\vartheta}\sqrt{\int_{X_0}^{X}\left[\bar{\vartheta} - \vartheta(x)\right]^2 \mathrm{d}x}; \qquad \bar{\vartheta} = \frac{1}{X - X_0}\int_{X_0}^{X}\vartheta(x)\mathrm{d}x. \tag{18}$$

Therefore, after integration, it results in

$$\Im \propto \frac{1}{S_\vartheta}\sqrt{(X - X_0)^3} = \frac{\sqrt{\ln^3(\tau/\tau_0)}}{S_\vartheta}. \tag{19}$$

The function $\Im$ depends on both τ and S_ϑ, so, its sudden change versus τ is related to the rate of change of S_ϑ. In fact, the total derivative of $\Im$ with respect to τ is

$$\frac{\mathrm{d}\Im}{\mathrm{d}\tau} = \Im\,(\tau, S_\vartheta)\left[\frac{3}{2\tau\,\ln^3(\tau/\tau_0)} - \frac{1}{S_\vartheta}\frac{\mathrm{d}S_\vartheta}{\mathrm{d}\tau}\right]. \tag{20}$$

The better useful condition for determining the onset of convection time is when $\Im$ reaches its maximum value at t_C, because in this case the onset time certainly falls within two consecutive measurements and its estimated uncertainty can be assumed as half the experimental resolution time Δt. So, from previous statements, the uncertainty in the onset of convection time determination could be similar to the estimated uncertainty in the Prandtl number or the thermal diffusivity. This occurrence imposes a minimum rate of change of S_ϑ at t_C given by

$$\left.\frac{\mathrm{d}S_\vartheta}{\mathrm{d}\tau}\right|_{\tau_C} \geq \frac{3}{2}\frac{S_\vartheta}{\tau_C\,\ln^3(\tau_C/\tau_0)}. \tag{21}$$

The rate of change of S_ϑ depends on the temperature measurement uncertainty, but also depends on fluid diffusion properties and experimental conditions such as the heat flux generated within the wire per unit length, the wire radius, and the position of the measurement zone along the wire. Preliminary rough measurements [11,13] performed on water ($Pr \approx 5$) and propylene glycol ($Pr \approx 400$), with a platinum wire diameter of 100 μm and an estimated value of 4 mK for S_ϑ, showed the condition imposed by Eq. 21 easy to obtain for several values of the heat flux generated per unit length and several vertical positions of the measurement zone along the wire.

Since the maximum dimensionless penetration distance depends on both the vertical position Z and the heat flux q generated per unit length (see Eq. 8), as an example, a preliminary value for the Prandtl number estimation (i.e., the kinematic viscosity divided by the measured thermal diffusivity) is reported using measurements performed on water and reported in Ref. [11], with a single measurement zone ($Z_{low,1} = 45.5$mm) and different heat fluxes, as shown in Fig. 4. The tests were executed at the undisturbed fluid temperatures in the range between 26.4 °C and 28.4 °C. In Fig. 4, after the correction for the radiation effect ($Kn^2 = 225.4\,\mathrm{m}^{-1}$), the dimensionless temperature difference $\vartheta - \vartheta_0$ is plotted versus the logarithm of the ratio between the measurement time t and the time t_0 when the influence of the wire heat capacity is negligible and ϑ increases as established by Eq. 17 (ϑ_0 is the value of the dimensionless temperature at t_0). By choosing the transient part in which the pure conduction regime is certainly present (linear trend of temperature versus the logarithm of time), the thermal properties of the fluid have been determined. The average estimated values of the thermal conductivity and thermal diffusivity were in this case $0.6\,\mathrm{W\cdot m^{-1}\cdot K^{-1}}$ and $0.143 \times 10^{-6}\,\mathrm{m^2\cdot s^{-1}}$, respectively.

The onset time t_C was determined by performing the F-test on the temperature differences shown in Fig. 4, searching for the time interval in which the absolute maximum value of the ratio $\Im$ between the expected and unexpected square residuals

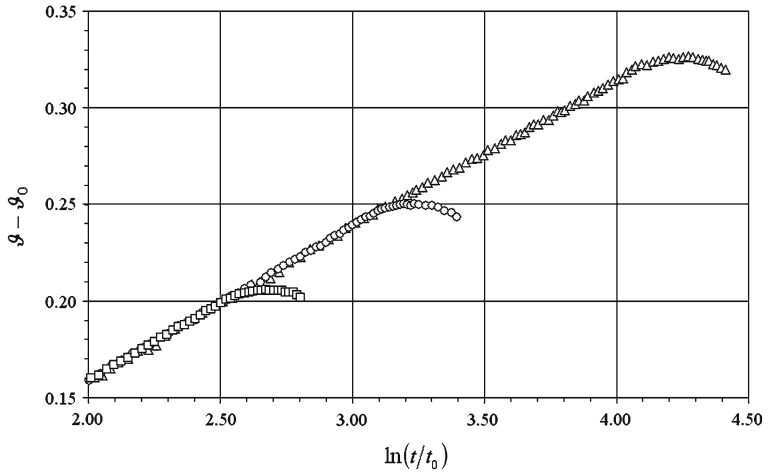

Fig. 4 Dimensionless temperature ϑ versus the logarithm of t/t_0 in the case of water for different heat fluxes generated: $q = 0.75\,\mathrm{W\cdot m^{-1}}$, $\vartheta_0 = 0.361$, and $t_0 = 0.715$ s (*triangles*); $q = 1.263\,\mathrm{W\cdot m^{-1}}$, $\vartheta_0 = 0.416$, and $t_0 = 1.43$ s (*circles*); $q = 1.885\,\mathrm{W\cdot m^{-1}}$, $\vartheta_0 = 0.442$, and $t_0 = 1.98$ s (*squares*)

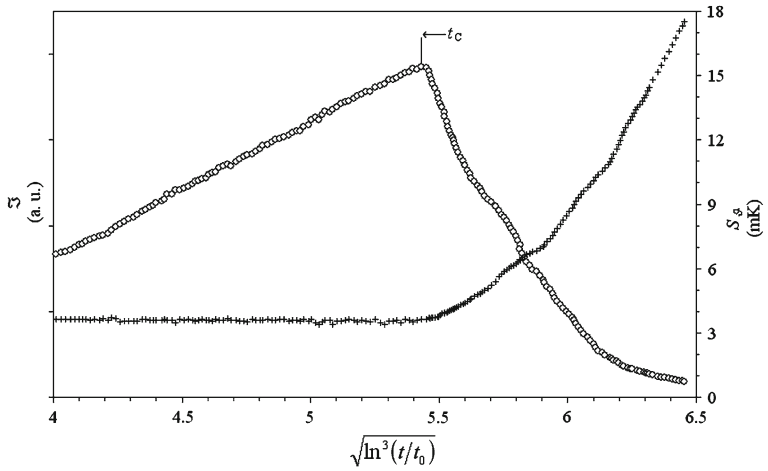

Fig. 5 Trend of the ratio $\Im$ between the expected and unexpected square residual (circles) and the unexpected standard deviation S_ϑ (crosses) determined from experimental measurements for the case of $q = 1.263\,\mathrm{W\cdot m^{-1}}$

is attained. In Fig. 5 both trends of $\Im$ and the unexpected standard deviation S_ϑ are plotted versus $\sqrt{\ln^3(t/t_0)}$ for the case of $q = 1.263\,\mathrm{W\cdot m^{-1}}$. In this plot, as expressed by Eq. 19, the trend of $\Im$ obtained experimentally is quite linear in the transient part driven only by conduction at constant S_ϑ. The absolute maximum value of $\Im$ is reached at $t_C = 31.4$ s, within a confidence region of about ± 1 s. For others tests performed with $q = 0.75\,\mathrm{W\cdot m^{-1}}$ and $q = 1.885\,\mathrm{W\cdot m^{-1}}$, in the same way, the calculated onset times t_C were 41.0 s and 24.9 s, respectively. For the proposed tests, the rela-

tive uncertainty u_{t_C} in determination of the onset time is about of 3 % on average. As expected, after the onset of convection, S_ϑ increases, $\Im$ decreases promptly, and the calculated rate of change of S_ϑ at t_C is one order of magnitude higher with respect to the minimum value required and imposed by Eq. 21. By a simple and preliminary approach, the approximated solution suggested by Eq. 12 can be used instead of Eqs. 8 and 9 for determination of the Prandtl number. The value of $\tilde{\zeta}$ corresponding to the vertical position of the lower potential lead, reached at the given time t_C by generating the heat flux q, is calculated using the left side of Eq. 12, with the estimated thermal diffusion properties of the fluid, and assigning a suitable value of the isobaric thermal expansion coefficient. Thus, the Prandtl number on the right side becomes a parameter to be estimated iteratively. With a constant value of $2.76 \times 10^{-4}\ \mathrm{K}^{-1}$ assigned for β at the average temperature of the tests (about 27 °C), the calculated average value of the Prandtl number is 5.3. Finally, taking into account the estimated value of the thermal diffusivity, the resulting kinematic viscosity is $0.758 \times 10^{-6}\ \mathrm{m}^2 \cdot \mathrm{s}^{-1}$. Although this value deviates by a few percent from values in the literature, by Eq. 16, with the estimated $u_{t_C} \approx 3$ %, the expected uncertainty in kinematic viscosity should exceed 10 %.

4 Conclusions and Future Activities

Early results from theoretical investigations of kinematic viscosity estimation by means of the hot-wire technique seem promising. By the introduced onset of convection time, the kinematic viscosity appears identifiable with a theoretical uncertainty of the same order as the estimated thermal diffusion properties by the hot-wire technique. Recent experiments performed on water and propylene glycol [11,13] confirm this result.

Since the onset of convection time is the essential parameter for identification of the fluid viscosity, future experiments have been planned and well focused on this target. Because the sensitivity on the onset time estimation by the hot-wire technique depends on the instantaneous rate of deviation from the typical temperature rise for the case of pure conduction, the onset convection time will be determined in the same experiment by both hot-wire and interferometric techniques. Since the fluid that is moving upwards introduces a vertical temperature gradient when it reaches a given position, this induces a sudden perturbation in the fringe pattern previously caused only by the variation of the refractive index in the radial direction. Setting up a kind of Twymann-Green interferometer, the wire surface will be used as a mirror, and by means of a cylindrical collimator, the laser beam will be squeezed and focused on the wire surface. The high sensitivity of the interferometer will allow comparisons of the estimated onset time by the hot-wire technique and validating this methodology.

References

1. J.H. Blackwell, Can. J. Phys. **34**, 412 (1956)
2. P.G. Knibbe, Int. J. Heat Mass Transf. **29**, 463 (1986)
3. V. Giaretto, M.F. Torchio, Int. J. Thermophys. **25**, 679 (2004)

4. C.A. Nieto de Castro, R.A. Perkins, H.M. Roder, Int. J. Thermophys. **12**, 985 (1981)
5. C.A. Nieto de Castro, S.F.Y. Li, G.C. Maitland, W.A. Wakeham, Int. J. Thermophys. **4**, 311 (1983)
6. L. Sun, J.E.S. Venart, R.C. Prasad, Int. J. Thermophys. **23**, 391 (2002)
7. R.J. Goldstein, D.G. Briggs, J. Heat Transf. Trans. ASME C **86**, 490 (1964)
8. J. Pantaloni, E. Guyon, M.G. Velarde, R. Bailleux, G. Finiels, Revue de Physique Appliqué **12**, 1849 (1977)
9. K. Velusamy, V.K. Garg, Int. J. Heat Mass Transf. **35**, 1293 (1992)
10. T. Lorenzo, J. Padet, Int. J. Heat Mass Transf. **45**, 2629 (2002)
11. V. Giaretto, E. Miraldi, M.F. Torchio, Rev. Sci. Instrum. **78**, 074901/1 (2007)
12. H.S. Carslaw, J.C. Jaeger, *Conduction of Heat in Solids*, 2nd edn. (Oxford University Press, London, 1959), pp. 341–342
13. V. Giaretto, Int. J. Mod. Phys. B **18**, 917 (2008)